



Computación y Sistemas

ISSN: 1405-5546

computacion-y-sistemas@cic.ipn.mx

Instituto Politécnico Nacional

México

Rueda, Aldo; Toledo, Miguel; Rueda, Fernando; Rangel, Rene
Numerical Investigation of the Droplet Behavior in Cascades Using a Finite Volume
Method
Computación y Sistemas, vol. 21, núm. 3, 2017, pp. 473-484
Instituto Politécnico Nacional
Distrito Federal, México

Available in: <http://www.redalyc.org/articulo.oa?id=61552758008>

- How to cite
- Complete issue
- More information about this article
- Journal's homepage in redalyc.org

redalyc.org

Scientific Information System

Network of Scientific Journals from Latin America, the Caribbean, Spain and Portugal

Non-profit academic project, developed under the open access initiative

Numerical Investigation of the Droplet Behavior in Cascades Using a Finite Volume Method

Aldo Rueda¹, Miguel Toledo², Fernando Rueda³, Rene Rangel⁴

¹ AMC Soluciones en Ingeniería,
Mexico

² Instituto Politécnico Nacional, SEPI-ESIME,
Applied Thermal and Hydraulic Engineering Laboratory,
Mexico

³ Universidad Veracruzana,
Research Centre for Sustainable Energy Resources,
Mexico

⁴ UNITEC, Estado de México,
Mexico

aldo_rueda2@hotmail.com, rrenerran@yahoo.com.mx

Abstract. This paper describes an Eulerian/Lagrangian two-phase model for wet steam. Two-dimensional inviscid transonic cascade flow is simulated using a cell-vertex finite volume space discretization method on structured triangular mesh. A pseudo time scheme is used to march the solution to steady state. The model provides an approach for including the interaction between the liquid and gas phases for a pure fluid. The analysis consists in the application of the discrete phase model, for modeling the liquid particle flow, and the Eulerian conservation equations to the continuous phase. The investigation permits us to know the influence of parameters such as: particle diameter, flow angle and particle velocity on deposition of drops onto stator blade surfaces. These parameters are analyzed to different inlet flow angles and drop sizes in the turbine. Deposition rate was found to be strongly dependent on increasing inlet flow angle and drop size in the example computed. The purpose of this paper is to present the results of some calculations of deposition which are based on more recent theories or less simplified flow models than previously published work.

Keywords. Cascade flow, finite volume method, steam turbines, two-phase flow, wet steam.

1 Introduction

Steam turbines play a dominant role in the generation of mains electrical supply and the

prospects of improved designs resulting from greater understanding are good [1]. The existence of the liquid phase in the low pressure (LP) steam turbines, formed by a polydispersed (different sizes) system of droplets, leads to loss of performance.

Additional energy losses, blade erosion and blade failures due to corrosion effects in the phase transition zone thus result in decreased turbine efficiency reliability [2]. This is attributed collectively to wetness losses, but the detailed mechanisms that give rise to these are insufficiently understood. In addition, the wetness loss is influenced by deposition rate, since it depends on the distribution of the total water content of the flow between fog drops and large drops (referred as coarse water) which are formed when deposited water is stripped from blade trailing edges.

A number of numerical studies, over the past several decades, have been directed toward modeling two-phase flow behavior of wet steam [3]. While Navier-Stokes solvers are needed to obtain accurate solutions for viscous flows in turbomachines, a fast Euler solver is still a desirable tool for routine applications particularly in problems, where viscous effects are confined to the walls regions. In this regard the numerical

approach most often used has been the inviscid-time marching scheme.

McDonald [3] was the first investigator to use the time marching, Finite Volume Method (FVM). Denton [4] extended McDonald's finite-volume method and has been used in inviscid viscous interaction programs for turbomachinery calculations. In these models the dispersed water phase can be handled via particle tracking along streamlines; this provides a wetness distribution (which is fundamental information for solving and minimizing the above wet steam effects in steam turbines) and hence mixture conditions for the subsequent single-phase inviscid flow calculation.

Young [5] reduced computational time and effort when he introduced a semi-analytical technique for investigating the thermal effects in wet-steam turbines, Ahmadi [6] simulated a two-dimensional inviscid transonic cascade flow using a cell-vertex finite volume space discretization method on unstructured triangular meshes. Qulan and co-workers in [2] proposed a numerical framework to study water drop erosion on turbine blades, it coupled fluid mechanics with solid mechanics.

In this work, inviscid flow is simulated by solving Euler equations on a purely triangular mesh using a time-marching solution method. The time dependent integral form of the equations is discretized in space using a cell-vertex FVM. Convergence acceleration is achieved by employing a polynomial smoothing. The governing equations, the discretization and the boundary conditions implementation are first presented. It is followed by the two-phase approach for modeling the interaction between the gas and liquid phases. The use of a two-phase approach has the potential for incorporating much more complex droplet models, since the two phases do not have to share the same velocity field.

2 Governing Equations and Discretization

Considering unsteady, inviscid two-dimensional compressible flow of a vapor carrying a population of droplets with no interphase slip, the continuity, momentum and energy equations, governing the

unsteady two-dimensional flow of an inviscid fluid (known as the Euler equations) are written in conservative form in a Cartesian coordinate system [7] as follows:

$$\frac{\partial U}{\partial t} + \frac{\partial F}{\partial x} + \frac{\partial G}{\partial y} = 0, \quad (1)$$

where U is a state vector of dependent variables and F and G are the flux vectors in the x and y directions, and are given by:

$$U = \begin{bmatrix} \rho \\ \rho u \\ \rho v \\ \rho E \end{bmatrix}, F = \begin{bmatrix} \rho u \\ \rho u^2 + p \\ \rho uv \\ \rho uH \end{bmatrix}, G = \begin{bmatrix} \rho v \\ \rho uv \\ \rho v^2 + p \\ \rho vH \end{bmatrix}. \quad (2)$$

Also it is needed the equation of state:

$$p = \rho \cdot R \cdot T \quad (3)$$

and for a polytropic process

$$\rho_k = \rho_1 \left(\frac{\rho_k}{\rho_1} \right)^n. \quad (4)$$

When the solution of steady flows is of interest it is assumed that the flow takes place at constant stagnation enthalpy and the energy equation is written as:

$$h_{tot} = \frac{k}{k-1} \cdot \frac{p}{\rho} + \frac{c_x^2 + c_y^2}{2} = const. \quad (5)$$

This assumption is exact when the flow becomes steady, even in the presence of shock waves.

For the scheme to be effective the equations must be solved in the order: mass-pressure-momentum. The order in which the momentum equations are solved is not important. The procedure adopted is to update the density from the continuity equation at all grid points then update the pressure from the equation of state. Finally, the new pressures together with the old densities and velocities are used to update the x momentum and y momentum. The method is therefore explicit [8], in the sense that the new variables are not used in the time step in which

they are calculated with the exception that the new pressure is used immediately it is available.

The boundary conditions applied at the downstream boundary are: a specified uniform static pressures and a condition of zero velocity gradient along the streamlines. At the upstream boundary the stagnation pressure and flow direction are specified.

A simple stability analysis has been developed for the scheme, and the maximum permissible time step can be calculated as:

$$(\partial t)_{CFL} \leq \left(\frac{|u|}{\partial x} + \frac{|v|}{\partial y} + \frac{|w|}{\partial z} + c \sqrt{\frac{1}{(\partial x)^2} + \frac{1}{(\partial y)^2} + \frac{1}{(\partial z)^2}} \right)^{-1}. \quad (6)$$

A homogeneous dispersed two-phase flow exists, in case the dispersed phase is distributed homogeneous in the continuous phase. The dispersed two-phase flow with steam as continuous phase and water droplets as the dispersed water is the essential part of the investigations in the present work. The volume fraction α_p is the ratio of the volume of the droplets to the total volume:

$$\alpha_p = \frac{V_p}{V_{Total}} \quad (7)$$

with V_p being the droplet volume.

The present model relies on a Lagrangian representation of the water droplet phase. The following describes how the Lagrangian tracking model was implemented for the cases of freshly nucleated and larger droplets. The motion model assumes the slip between the droplet and the surrounding gas.

This is a reasonable assumption considering that the radius of a freshly nucleated droplet may grow to a size in the range of 10^{-7} m within the extent of the solution domain [9]. The method used in this work is based on the calculation of the path of several individual solid particles through the flow field. Each particle represents a sample of particles that follow an identical path. The motion of the tracked particles is taken to describe the average behavior of the discrete phase. While setting up the Lagrangian tracking and the deposition model described below, the following assumptions have been made according to Ahmadi in [6]:

- Particle-particle interactions are neglected;
- Only spherical, non-reacting and non-fragmenting particles are considered.

We do consider, according to Ulrichs [10]:

Change of the continuous trajectory due to the effect of the discrete phase trajectories on the continuum (this is a condition for monitoring erosion).

We need to specify, according to Mashmouhy in [11]:

- Starting positions, velocities of each particle stream (relative velocities if moving framed is used);
- Diameter of the particle;
- Mass flow rate of the particle stream that will follow the trajectory of the individual particle (droplet).

The particles are injected and tracked through a network of flux-elements. The gas-phase equations are solved at the control-volume locations. When a particle is injected into the flow (for steady-state calculations) the particle is tracked until some fate is reached, such as impacting a wall, passing into a periodic boundary or exiting the flow domain. For a particular fate, a predetermined action is undertaken such as leaving the domain (outflow), translation and reinjection (periodic condition) and collection [12].

During a particle's journey to a particular fate it will pass through a succession of flux-elements, and the inertia force of a particle in a gas flow is in equilibrium with all forces acting on the particle:

$$m_p \frac{d \bar{v}_p}{dt} = \frac{\pi}{6} D_p^3 \rho_p \frac{d \bar{v}_p}{dt} = \sum_i \bar{F}_i. \quad (8)$$

The forces F_i include the drag force, $F_D (v - v_p)$, and the force required to accelerate the fluid surrounding the particle with diameter D_p , mass m_p , density ρ_p and velocity v_p . This model permits us to simulate a discrete second phase in a Lagrangian frame of reference, where the second phase consists of spherical particles dispersed in the continuous phase.

In what follows, all distances are non-dimensionalized (except droplet deposition rate)

using an appropriate characteristic length and all flow variables are non-dimensionalized as follows:

$$\begin{aligned} P &= \frac{p}{\rho_1 a_1^2 M_1}, \\ \sigma &= \frac{\rho}{\rho_1}, \\ U &= \frac{\rho c_x}{\rho_1 c_1}, \\ V &= \frac{\rho c_y}{\rho_1 c_1}. \end{aligned} \quad (9)$$

A cell-vertex finite volume method is used to discretize the equations of motion, eq. (1), on a structured triangular mesh. The computational domain is divided into triangles, fixed in time, and the flow variables are stored at their vertices. For any node, the control volume (surface in 2D) is taken as the union of all triangles with a vertex at that node, i. e. the control volumes are overlapping.

The governing equations, eq. (1), are then integrated over each control volume Ω (surface in 2D) which is bounded by the surface $\partial\Omega$ (curve in 2D), and using Gauss theorem (Green's theorem in 2D) one obtains:

$$\frac{\partial}{\partial t} \iint_{\Omega} R dx dy + \int_{\partial\Omega} (F dn_x + G dn_y) = 0. \quad (10)$$

The fluxes F and G along a particular edge of the control volume are numerically evaluated as the average of the nodal flux values at the ends of that edge. When the cell-vertex discretization scheme is applied to eq. (10), we get the following set of equations for each cell i :

$$\frac{\partial}{\partial t} (S_i R_i) + \sum_{e=1}^n (F_e n_{xe} + G_e n_{ye}) = 0, \quad (11)$$

where the summation is taken over all edges of cell i . S_i is the cell area, R_i is the solution vector, F_e and G_e are the components of the flux vector on edge e , and n_{xe} , n_{ye} are the components of the outward normal to edge e . when eq. (11) is written for all cells i , we get:

$$\frac{\partial}{\partial t} (S_i R_i) + Q(R_i) = 0, \quad (12)$$

where $Q(R_i)$ represents the discrete approximation to the convective flux integral.

3 Computational Method

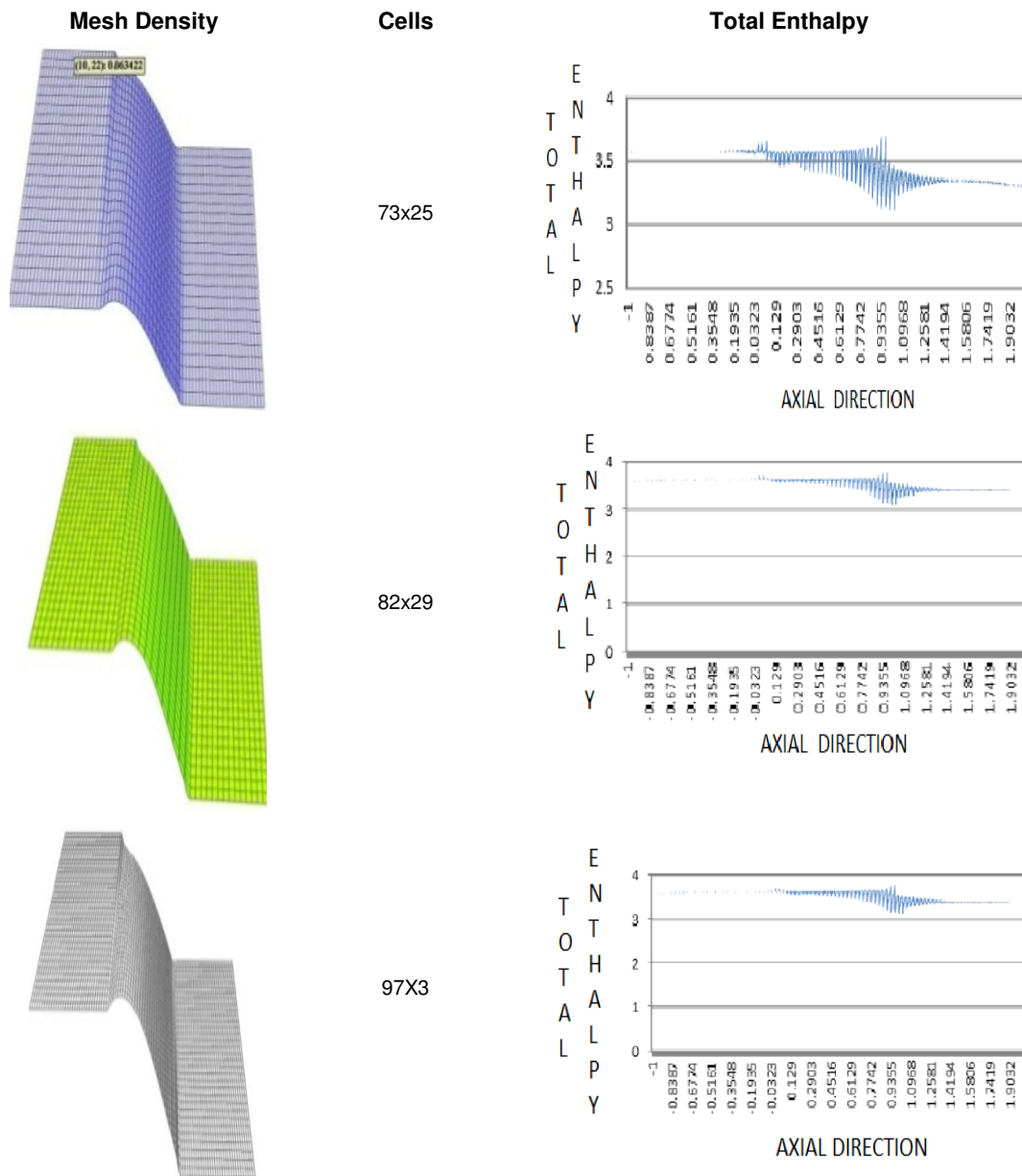
A two-dimensional wet steam flow is described by the system of Eulerian/Lagrangian equations in which the conservation equations of gas dynamics were solved in Eulerian formulation while the liquid phase was treated in Lagrangian coordinates. This model allows the droplet integration to be separated from the grid size, and gas phase time step, allowing for a coarser grid to be employed. Since each droplet size is integrated from its initial creation to a final fate, no special handling is required to account for movement through a wide range of size regimes.

Time marching methods are in principle the most flexible means of calculating blade-to-blade flows in turbomachinery since the same method can be used for subsonic, transonic and supersonic flows with automatic inclusion of time dependence. The basic principle of time marching is to start with a guess flow distribution and integrate the time dependent equations of motion forward with time until a steady-state solution is obtained.

The concept chosen was to use McDonald's elemental control volume but with an H grid. The mesh is formed by a series of quasi-streamlines which are evenly spaced in the y direction and by pitchwise direction lines which need not be evenly spaced in x direction.

The quasi-streamlines upstream and downstream of the cascade are chosen to be roughly in line with the flow inlet and outlet directions but these lines do not control the flow direction. The outlet flow direction is obtained as part of the calculation being determined by the periodicity condition behind the trailing edge. Periodic boundaries are treated in the same way as solid boundaries but after each time step the properties at corresponding points are averaged.

The computational code was structured in three parts: the first program produces the two dimensional finite mesh system of turbine cascade and the input data are: profile length, staple angle and number of original profile coordinates.

Table 1. Mesh refinement on the blade surface

The second program calculates the density and momentum distributions of 2-dimensional transonic potential flow by time step method at turbine cascade, the input data are: x and y – axial mesh coordinates, upstream velocity, upstream pressure, downstream pressure, upstream density, upstream flow angle, isentropic exponent,

efficiency of turbine cascade, time segment; the third program obtains the drop trajectories and humidity distributions of two dimensional turbine cascade.

Relevant input data are: radius of particle, density of particle, dynamic viscosity and upstream humidity.

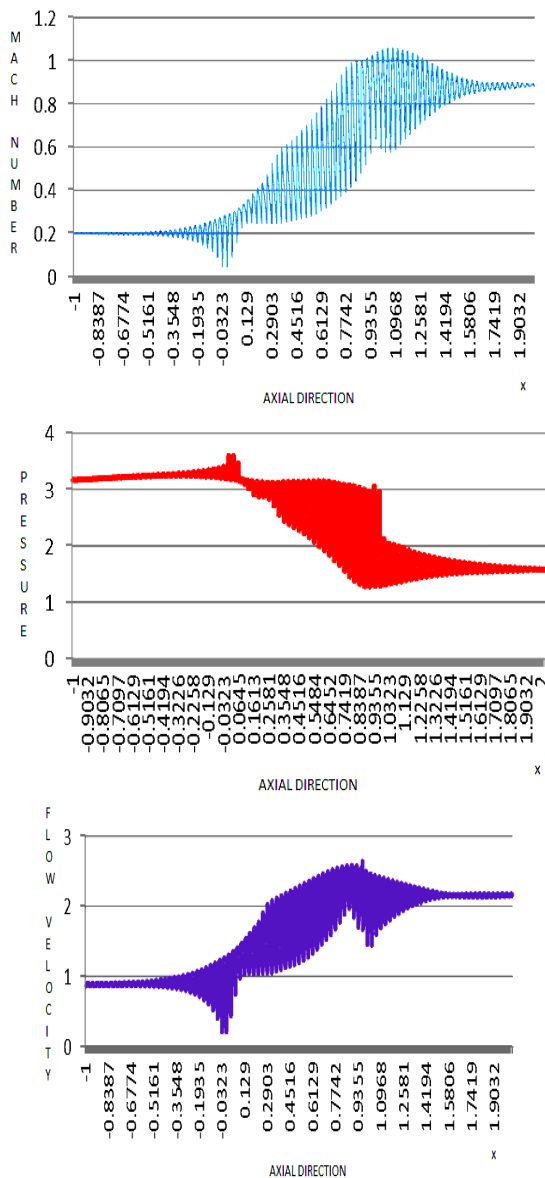


Fig. 1. The contours of Mach number, pressure and velocity in the passage at mid-plane (dimensionless), $\beta_1 = 90^\circ$

3.1 Stator Blade Turbine Cascade

The test case is the transonic flow of an experimental impulse turbine stator channel. At inlet, the steam angle is 54° , steam pressure is 4

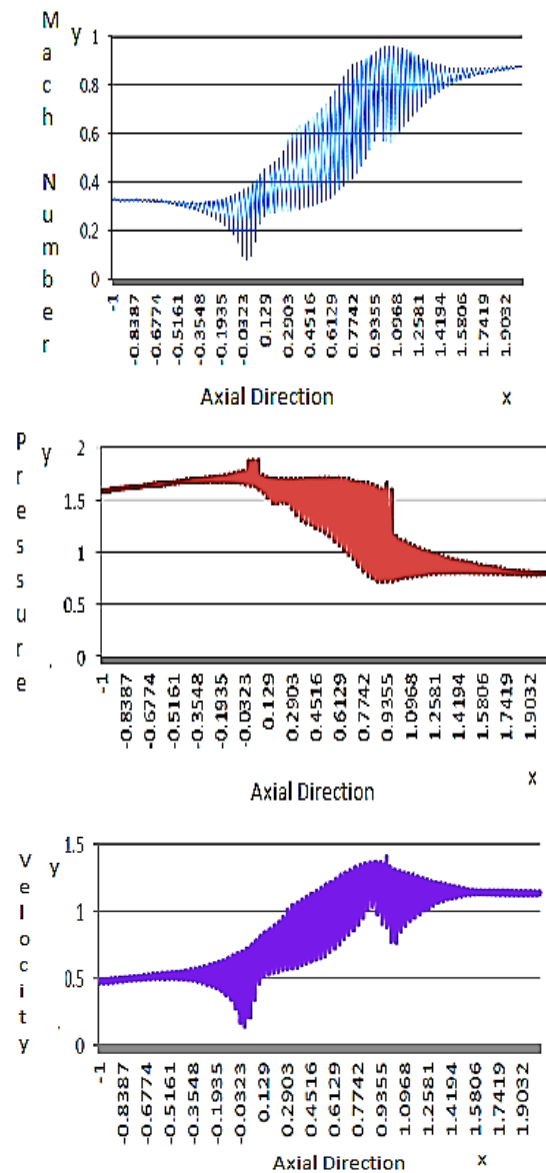


Fig. 2. The contours of Mach number, pressure and velocity in the passage at mid-plane (dimensionless), $\beta_1 = 120^\circ$

kPa, steam density is 0.02873 kg/m^3 , steam velocity is 100 m/s ; at outlet, the steam pressure is 2 kPa . The ratio of pitch to blade chord length is 0.9 . The initial entrained wetness fraction is 7.0% and there are no relative velocities between

phases at the starting position. While setting up the Lagrangian tracking [13], the following assumptions have been made: particle-particle interactions are neglected, any change of the flow turbulence caused by the particles is not accounted for, only spherical particles are considered and the geometry modifications have been neglected.

This means that the computational model geometry during simulation was invariable [14]. The drops are homogeneous distributed at inlet and the flow angle is taken to be uniform. The FVM solver described in section 2 is validated against the experimental test case namely impulse cascade.

4 Results

A series of results is presented, which includes the simulations carried out with the stator configuration. At inlet, the relative flow angle varies from 90° to 120° , and the Mach number varies from 0.23 to 0.28. The numerical analysis was conducted using a computational algorithm coded in Fortran 90 on the basis of finite volume method. Table 1 summarizes the analyses of grid sensibility, showing the results on grid refinement on the blade surface.

A converged solution was obtained for a base running ($\beta_1 = 90^\circ$) in 14 491 iterations and a base running ($\beta_1 = 120^\circ$) in 12 068 iterations. The inlet fluxes are $2.509 \text{ kg/m}^2\text{s}$ and $3.4827 \text{ kg/m}^2\text{s}$. The convergence criterion for continuity and momentum equations was set in levels of $1\text{E-}3$. Figs. 1-2, show numerical results obtained by the simulation for each base running. They show the contours of Mach number, pressure and velocity distribution at mid-span (50% vane height) passage.

The numerical and analytical Mach number distributions along the suction and pressure surfaces, plotted in Figs. 1 and 3, are in good agreement.

Fig. 4 represents the particle tracks released from the inlet domain, they show particle tracks and path lines for each base running.

Fig. 5 represents the velocity profiles of wet steam in the passage, the orange dot line reach the highest velocity value before the other dot lines. It

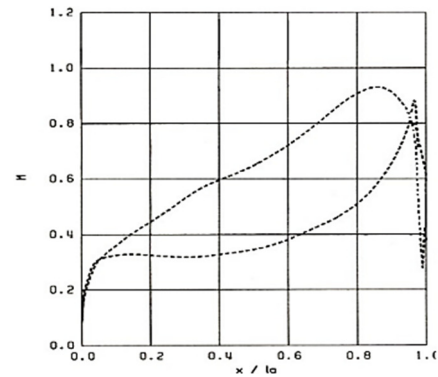


Fig. 3. Analytical Mach number distribution for stator blade cascade

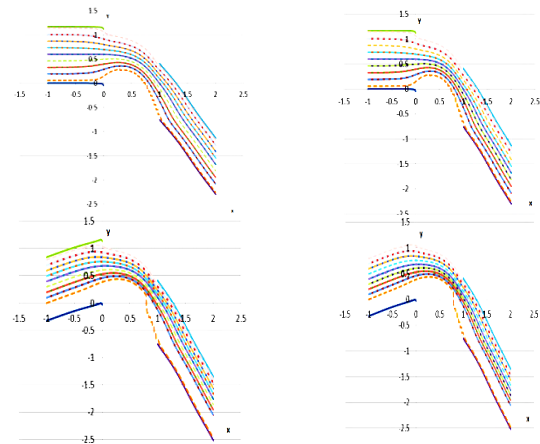


Fig. 4. Particle tracks and paths lines for base running (left), profile of velocity against position (right)

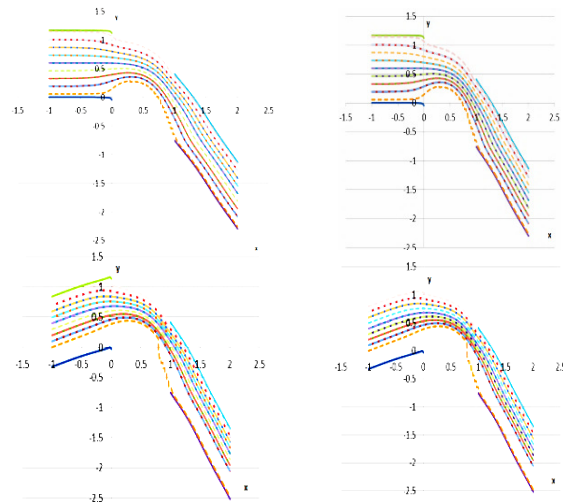


Fig. 5. Velocity profiles of wet steam in the passage

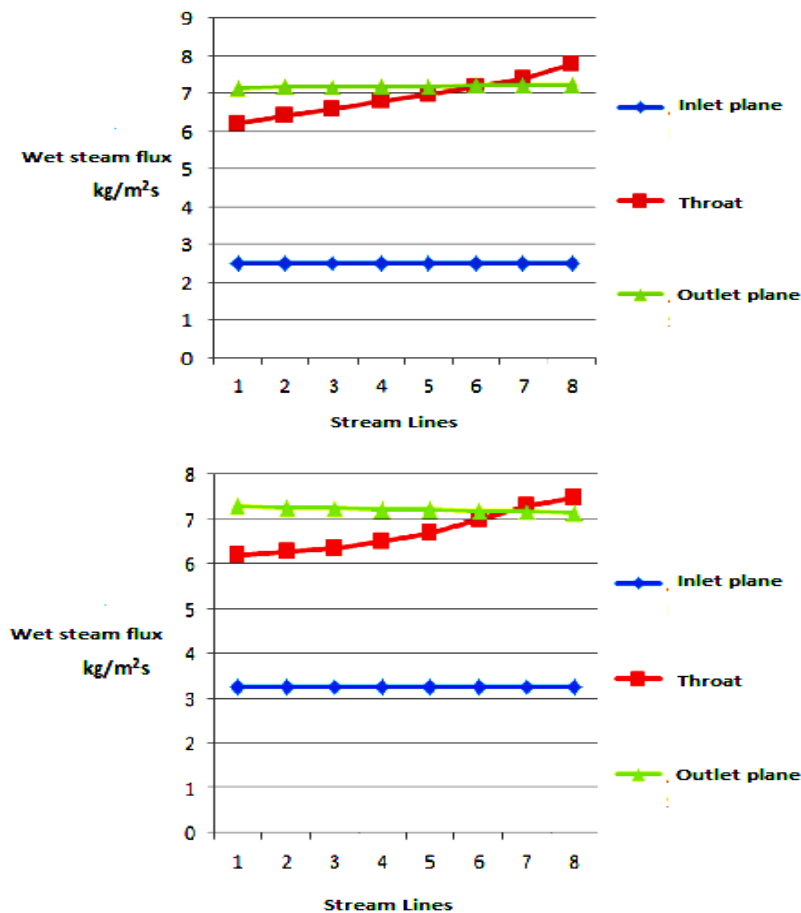


Fig. 6. Wet steam flux on stator blade surfaces

represents the particle trajectory closer to the suction side and matches the orange dot line

Fig. 6 illustrates the stability of computational calculation for wet steam flow in three sections of the channel. The flux increases in the zone of the throat where there is a change in geometrical and flow conditions then stability is almost achieved in the outlet plane.

The areas in which moisture distributes along the pitch are shown in fig. 7 and 8.

5 Discussion

The FVM solver described is a mathematical and computational model that simulates the trajectories and velocities of water drops, as well as the

distribution of mass of the particles. The numerical solution shows the maximum steam flow velocities reach 280 m/s ($\beta_1 = 90^\circ$) and 275.51 m/s ($\beta_1 = 120^\circ$) in the throat passage. The minimum value is in the leading edge, which corresponds to the stagnation point. The pressure distributions at the mid span are shown in figs. 1 and 2. The maximum pressure on the leading edge has a value of 3.98 kPa ($\beta_1 = 90^\circ$) and 4.049 kPa ($\beta_1 = 120^\circ$), while the minimum is on the suction side in the throat region, see Table 2.

Variations in steam flow angle and diameter of the particles were done to predict the quantity and distribution of the deposited water on stator blade surfaces. The concave surface of a blade can collect droplets by inertial impact; shown in Figs. 7 and 8.

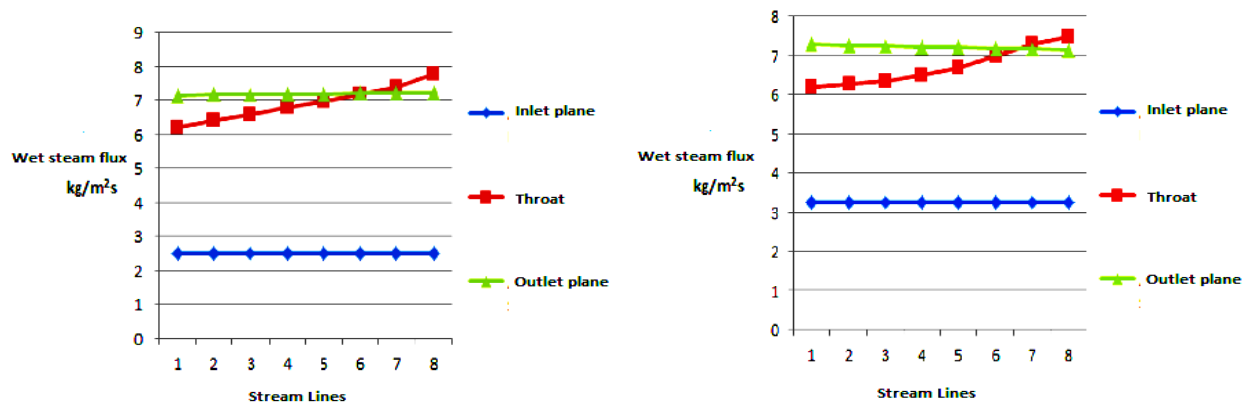
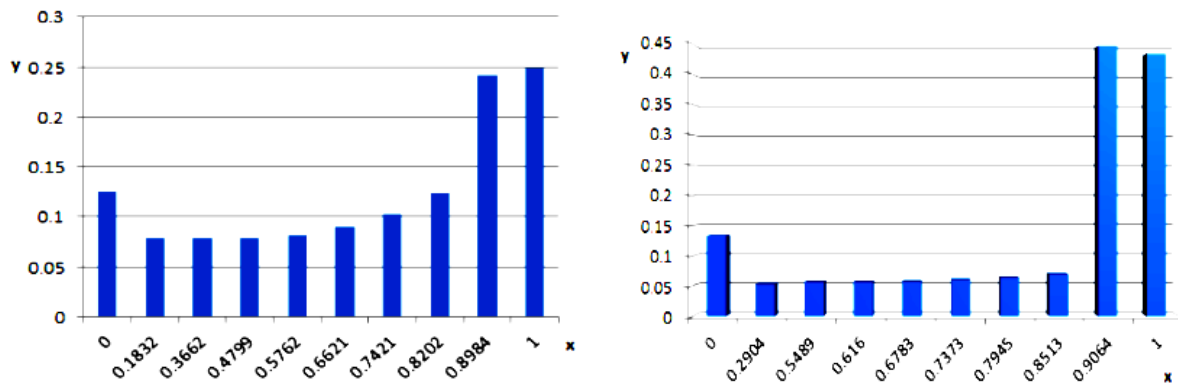
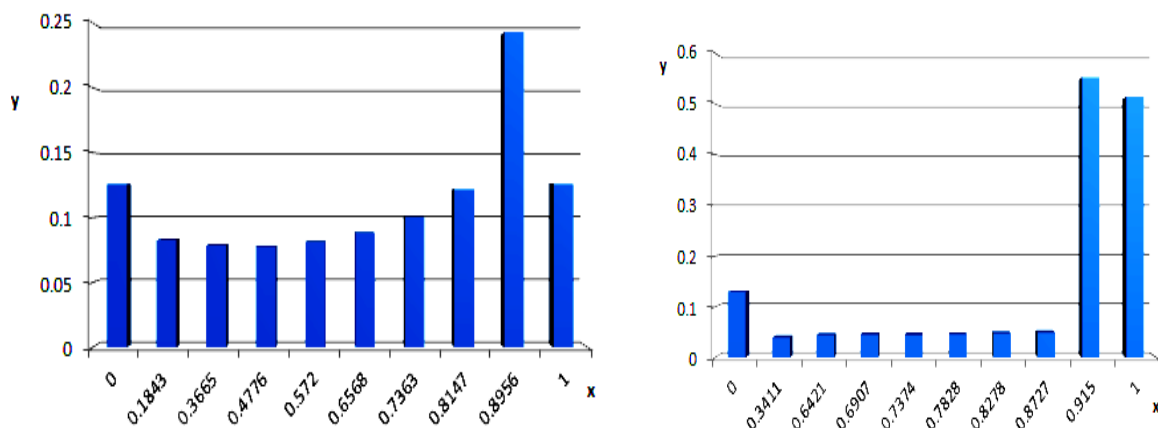


Fig. 6. Wet steam flux on stator blade surfaces

Fig. 7. Deposition as a function of pitch distance – x direction (dimensionless) in stator blades, $d_p = 0.25 \mu\text{m}$, $\beta_{1\text{left}} = 90^\circ$, $\beta_{1\text{right}} = 120^\circ$ Fig. 8. Numerical data of deposition as a function of pitch distance – x direction (dimensionless) in stator blades., $d_p = 1.0 \mu\text{m}$, $\beta_{1\text{left}} = 90^\circ$, $\beta_{1\text{right}} = 120^\circ$

This effect was modeling taking the streamlines to be parabolic with a constant velocity component in the direction of the inlet flow as shown in Fig. 4. Ignoring the boundary layer, a numerical result was obtained for the collection of droplets in terms of direct inertia impaction.

The diameter changes from 0.25 μm up 1 μm . Most 0.25 μm particles move along with the steam flow consistently, and very few particles impact de inner arc of blade. When the inlet angles of flow are different, more 0.25 μm particles tend to impact the stator blade under the full load. By contrast, with the dominance of their inertia, 1 μm particles can be easily separated from steam flow and impact the stator blade surface at a high normal velocity [15].

As the diameter of the liquid particles increases, the deposition rate also increases reaching a maximum value near the trailing edge in the axial direction. The water deposition rises, changing from 6.0749 $\text{kg/m}^2\text{s}$ to 7.5 $\text{kg/m}^2\text{s}$ at the exit, this performance is caused by the fact that as diameter, flow angle and velocity increase, the amount of deposited particles increases.

Fig. 6 presents the curves of droplet deposition rate for the base running at each case. It is observed that maximum value is located at the trailing edge, see Table 3. This value reaches 7.92 $\text{kg/m}^2\text{s}$ and corresponds to the throat zone. In the leading edge the deposition rate is minimum compared with the throat zone, near to 2.5 $\text{kg/m}^2\text{s}$.

By comparison, Q. Zhou, Na Li and co-workers [16] established a numerical framework that analyzed the movements of water drop in a blade channel based on the solution of the flow field of water steam in turbine, and statistics such as velocity and position were obtained as the working condition and particle size was varied. They developed a numerical tool to study the water drop erosion in turbine engines. Computational fluid dynamics and particle trace model in the Lagrangian Coordinates were employed to simulate the trajectories of water drop in a flow of wet steam in the blade channel.

6 Conclusions

The predictions reported in this paper contain the modeling of flow with changes of inlet parameters.

Table 2. Steam flow parameters

Relative flow angle β_1 , inlet	Velocity (throat passage) m/s	Pressure kPa	Inlet fluxes $\text{kg/m}^2\text{s}$
90°	280	3.98	2.509
120°	275.51	4.049	3.4827

Table 3. Deposition parameters

Drop diameter μm	Humidity (%), $\beta_1 = 90^\circ$	Humidity (%), $\beta_1 = 120^\circ$	Maximum deposition rate $\text{kg/m}^2\text{s}$
0.25	2.5	4.5	7.92
1.0	275.51	4.049	7.5

The objective was to modify the existent flow a pattern, looking to understand the mechanism through which erosion and wetness loss develops and minimize their impact on blade surfaces. In the present work continuous-discrete phase model was used to predict the water deposition distribution on surface stator blades. Two-dimensional inviscid transonic flow was simulated using a cell-vertex finite volume space discretization method on structured triangular mesh. The steady state solution was reached by pseudo-time marching the Euler equations. Polynomial smoothing was used for convergence acceleration.

The effect of vapor mass flow rate, flow angle and diameter of the particle are studied by comparing the results, obtained by solving CFD problem.

The comparison shows that the effect of the variation of these parameters increases the deposition mechanism. The deposition distribution obtained varying flow angle and diameter of particles show that the values of surface deposition increase, while the drop diameter increases. The distribution of droplet deposition is fundamental information for solving and minimizing the wet steam effects in the steam turbines. Knowledge of the quantity and distribution of the deposited water is necessary if the operating life of the moving

blades in a given turbine is to be predicted with any accuracy.

(CONACyT) and Instituto Politécnico Nacional (IPN).

Appendix 1. Conventions

a	Speed of sound; [m/s],
c	Absolute velocity; [m/s],
c_x	Axial velocity of the blade; [m/s],
c_y	Tangential velocity of the blade; [m/s],
D	Droplet diameter; [μm],
F	Force; N,
h	Enthalpy; [kJ/kg],
k	Isentropic Coefficient; [-],
m_p	Droplet mass; kg,
M	Mach Number; [-],
p	Pressure; [Pa],
t	Time; [s],
V_p	Droplet Volume; [m^3],
v_p	Droplet velocity; [m/s],
x	Axial coordinate, [-]
y	Tangential coordinate; [-],

Greek Letters

α_p	Volume fraction
β	Relative angle respect to the tangential axis
ρ	Density; [kg/m^3],

Subscripts

1	Inlet
2	Outlet
a	Axial component
e, i	Cell number
k	Surrounded point
p	liquid phas

Acknowledgements

The authors would like to thank the Applied Thermal and Hydraulic Engineering Laboratory that provided the authors with facilities and equipment. This work was supported by the Consejo Nacional de Ciencia y Tecnología

References

1. **Backhtar, F., Rassam, S.Y., & Zhang, G. (1999).** On the performance of a cascade of turbine rotor tip section blading in wet steam Part 4: droplet measurements. *Journal of Mechanical Engineering Science*, Vol. 213, No. 4, pp. 343–353.
2. **Qulan, Z., Na, Li., Xi, C., & Tongmo, X. (2009).** Analysis of water drop erosion on turbine blades based on a nonlinear liquid-solid impact model. *International Journal of Impact Engineering*, Vol. 36, No. 9, pp. 1156–1171. DOI: 10.1016/j.ijimpeng.2009.02.007.
3. **McDonal, P. W. (1971).** The computation of transonic flow through two-dimensional gas turbine cascades. *ASME Gas Turbine Division*, Vol. 71, pp. 3–6.
4. **Denton, J. D. (1975).** A time marching method for two and three dimensional blade to blade flows. *Aeronautical Research Council*, Vol. 3775, pp. 2–25.
5. **Young, J. B. (1984).** Semi analytical techniques for investigating thermal non equilibrium effects in wet steam turbines. *International Journal of Heat and Fluid Flow*, Vol. 5, No. 2, pp. 81–91. DOI:10.1016/0142-727X(84)90026-2.
6. **Majid, A. & Wahid-Ghaly, S. (1997).** Simulation of inviscid flow in cascades using a finite volume method with solution adaptation. *Proceedings of aerodynamics symposium*, Vol. 6, pp. 213–222.
7. **Gerber, A. G. (2002).** Two Phase Eulerian/Lagrangian model for nucleating steam flow. *Journal of Fluids Engineering*, Vol. 124, No. 2, pp. 465–475. DOI: 10.1115/1.1454109.
8. **Denton, J. D. & Dawes, W. N. (1999).** Computational fluid dynamics for turbomachinery design. *Journal of Mechanical Engineering Science*, Vol. 213, No. 2, pp. 107–124. DOI: 10.1243/0954406991522211.
9. **Gerber, A. G. & Mousavi, A. (2007).** Representing polydispersed droplet behavior in Nucleating Steam Flow. *Journal of Fluids Engineering*, Vol. 129, No. 11, pp. 1404–1414. DOI:10.1115/1.2786536.
10. **Mazur, Z., Urquiza, G., Sierra, F., & Campos, R. (2002).** Numerical analysis of erosion of the rotor labyrinth seal in a geothermal turbine. *Geothermics*, Vol. 31, No. 5, pp. 563–577. DOI: 10.1016/S0375-6505(02)00014-7.

11. **Ulrichs, S. (2007).** *Experimental investigations in the behavior and influence of water droplets in a compressor cascade flow.* Department of Mechanical Engineering of the Helmut-Schmidt-University, pp. 17–39.
12. **Mashmouhy, H., Mahpeykar, M. R., & Bakhtar, F. (2004).** Studies of nucleating and wet steam flows in two-dimensional cascades. *Journal of Mechanical Engineering Science*, Vol. 218, No. 8, pp. 843–858.
13. **Crane, R. I. (1982).** Drop coalescence and deposition in turbulent wet steam pipe flows. *International Journal of Heat and Fluid Flow*, pp. 313–320.
14. **Mazur, Z., Campos-Amezcu, R., Urquiza-Beltran, G., & García-Gutiérrez, A. (2004).** Numerical 3D simulation of the erosion due to solid particle impact in the main stop valve of a steam turbine. *Applied Thermal Engineering*, Vol. 24, pp. 1877–1891.
15. **Awatef, A.H., Widen-Tabakoff, R.B., Rivir-Kaushik, D., & Puneet, A. (2005).** Turbine Blade Surface Deterioration by Erosion. *J. Turbomach*, Vol. 127, pp. 445–452.
16. **Qulan, Z., Na, L., Xi, C., Yonezu, A., Xu, T., Hui, S., & Di, Z. (2008).** Water Drop Erosion on Turbine Blades: Numerical Framework and Applications. *Materials Transactions*, Vol. 49, pp.1606–1615.

*Article received on 11/02/2016; accepted on 13/03/2017.
Corresponding author is Aldo Rueda.*